

Dynamic Interference Prediction for In-X 6G Sub-networks

Pramesh Gautam*, Ravi Sharan B A G[†], Paolo Baracca[‡], Carsten Bockelmann*, Thorsten Wild[†], Armin Dekorsy*

*Department of Communications Engineering, University of Bremen, Germany,

Email: {gautam, bockelmann, dekorsy}@ant.uni-bremen.de

[†]Nokia Bell Labs Stuttgart, Germany, Email: {ravi.sharan, thorsten.wild}@nokia-bell-labs.com

[‡] Nokia Standards, Munich, Germany, Email: paolo.baracca@nokia.com

Abstract—The sixth generation (6G) industrial Sub-networks (SNs) face several challenges in meeting extreme latency and reliability requirements in the order of 0.1 – 1 ms and 99.999-to-99.99999 percentile, respectively. Interference management (IM) plays an integral role in addressing these requirements, especially in ultra-dense SN environments with rapidly varying interference induced by channel characteristics, mobility and resource limitations. In general, IM can be achieved using resource allocation and *accurate* Link adaptation (LA). In this work, we focus on the latter, where we first model interference at SN devices using the spatially consistent 3GPP channel model. Following this, we present a discrete-time dynamic state space model (DSSM) at a SN access point (AP), where interference power values (IPVs) are modeled as latent variables incorporating underlying modeling errors as well as transmission/protocol delays. Necessary approximations are then presented to simplify the DSSM and to efficiently employ the extended Kalman filter (EKF) for interference prediction. Unlike baseline methods, our proposed approach predicts IPVs solely based on the channel quality indicator (CQI) reports available at the SN AP at every transmission time interval (TTI). Numerical results demonstrate that our proposed approach clearly outperforms the conventional baseline. Furthermore, we also show that despite predicting with limited information, our proposed approach consistently achieves a comparable performance w.r.t the off-the-shelf supervised learning based baseline.

Index Terms—6G, Interference Prediction, Network-of-Networks, Link Adaptation, Sub-Networks, 3GPP, HRLLC.

I. INTRODUCTION

There is an increasing demand to integrate emerging vertical industry use cases as part of the future sixth generation (6G) communication infrastructure. The “Network-of-Networks” concept has been identified as a potential solution, where a vertical can be integrated as a sub-network (SN) [1]. A typical SN consists of an access point (AP) and several user equipments (UEs) either connected to the AP or communicating among themselves. Moreover, these SNs are envisaged to operate either in a fully-autonomous fashion or under the purview of a larger network. We refer to [2] for example SN use-cases and deployment scenarios.

This work is supported by the German Ministry of Education and Research (BMBF) under the grants of 16KISK109 (6G-ANNA) and 16KISK016 (Open6GHub).

Interference management (IM) has been identified as one of the major technical challenges involved in real-time SN deployments. From an air-interface perspective, IM can be achieved through a combination of resource allocation and link adaptation (LA). While the former focuses more on appropriate radio resource management, IM through LA involves exploiting the underlying transmission link characteristics. In this work, we focus on improving the LA aspects of IM for *In-X* SNs. The In-X SNs are a special category of SNs targeting short-range communications with hyper-reliable, low-latency communication (HRLLC) traffic with latency and reliability requirements ranging between 0.1 – 1 ms and 99.999-to-99.99999 percentile, respectively [3].

A straight-forward LA scheme used for existing ultra-reliable, low-latency communication (URLLC) traffic involves modulation and coding scheme (MCS) selection based on the channel quality indicator (CQI) report and acknowledgement (ACK)/non-acknowledgement (NACK) feedback. Here, CQI report is a quantized information characterizing the transmission link and the effective interference perceived at a UE. Such a scheme is not readily applicable for IM in SNs for the following reasons. Firstly, short packets of HRLLC traffic occupy only a fraction of the physical resources in a transmission time interval (TTI) compared to URLLC traffic. This results in a rapid variation of interference among SNs, which can be particularly challenging to track in real-time. Added to this, the delay involved in the CQI reporting mechanism [4] only makes it worse. Secondly, extreme low latency requirements of SNs impose stringent limitations on packet retransmissions — oftentimes limiting it to only one retransmission. Such requirements cannot be met with the LA scheme described above due to ultra-dense SN deployments.

Several inference tools have been investigated in the literature for improved interference representation in the CQI report and subsequently in the LA schemes. These methods can be classified as either UE-side or AP-side improvements. In [5], UE-side CQI adjustments are proposed, where low-pass filtered interference estimates are factored into signal to interference plus noise ratio (SINR) estimates. Similarly, the authors in [6] propose several UE-side Gaussian kernel-

based interference prediction methods. A drawback of [5] and [6] is that these works assume that the channel estimates of interfering devices are readily available at the UEs. The works in [7] and [8] demonstrate a superior prediction error performance by using a long short-term memory (LSTM) and federated-learning based UE-side interference prediction for an In-X SN scenario with deterministic traffic. While the explicit need for channel estimates is relaxed in [7] and [8], labels or ground-truth interference power values (IPVs) used for training the neural networks can be hard to obtain in reality due to the additional communication overhead in ultra-dense scenarios. In general, UE-side methods improve the interference representation in the CQI report; however they still do not account for transmission and protocol delays involved. Moreover, the battery limitations usually pose a computational bottleneck for the UE-side approaches.

For the AP-side methods, the authors in [9] model the IPVs using a discrete-time Markov chain and use a moving-average filter based predictor for improving the resource allocation aspects of IM. While not primarily an interference prediction mechanism, [10] proposes two CQI prediction methods based on Wiener filter and cubic spline extrapolation, while accounting for several modeling errors involved in obtaining the CQI report. A common drawback of the existing literature is that interference/SINR prediction mechanisms only consider the tail probabilities of the underlying probability density function (pdf). This can be challenging to formally characterize IPVs correlated across time and oftentimes lead to an oversimplification of the LA problem.

In this work, we propose an AP-side low-complexity on-line interference prediction method performed w.r.t the SN data transmissions. More specifically, we employ an extended Kalman filter (EKF)-based predictor to obtain IPV estimates from the CQI report to ultimately improve the LA. To the best of our knowledge, AP-side methods exploiting the interdependencies between the CQI report and IPVs have not been explored in either SN or HRLLC literature before. The main contributions of this work are summarized below:

- 1) We formally characterize the inter-SN interference following the spatially consistent third generation partnership project (3GPP) channel model and an ON-OFF traffic model.
- 2) We present a discrete-time Gaussian dynamic state space model (DSSM), where the IPVs are modeled as hidden/latent state with CQI report as the corresponding observations. We also present the relevant simplifications of the DSSM to efficiently employ the EKF. An advantage in using the DSSM is that the range of IPVs is not just restricted to tail pdf.
- 3) Finally, we corroborate our proposed approach with the help of numerical results. We show that the proposed method can achieve a comparable performance w.r.t the Genie LA baseline. In contrast to other methods it is performed solely based on the available CQI reports as observations and without any explicit feedback/labels.

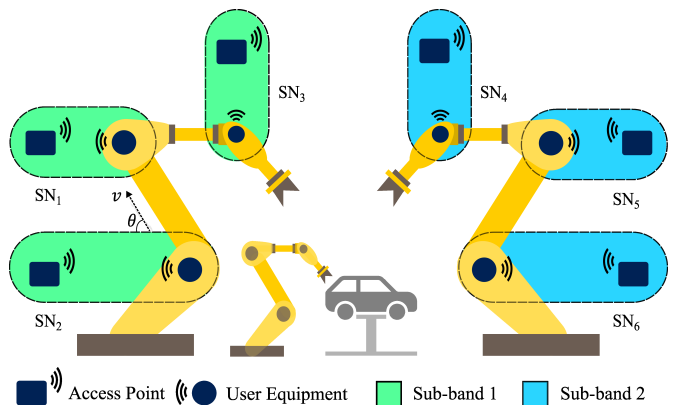


Fig. 1: Example In-X SN scenario in an automobile assembly unit. Here, several APs communicate with associated sensor-actuator pairs acting as UEs.

II. SYSTEM MODEL

Let $\mathcal{N} = \{1, 2, \dots, N\}$, $|\mathcal{N}| = N$, denote the set of In-X SNs distributed according to a uniform random variable in a confined area \mathcal{A} . Each SN $n \in \mathcal{N}$ consists of a single AP serving a single UE in the downlink (DL)¹. Since an AP uniquely identifies a SN, the terms SN and AP are used interchangeably in this paper. Each SN is assumed to be moving with constant velocity v with the direction defined by $\theta \in [0, 2\pi]$ (see Fig. 1). Moreover, SNs are configured to maintain a minimum separation distance.

We assume a slotted time operation where each slot or a TTI is denoted by $t \in \mathbb{N}$. Furthermore, the slot duration is assumed to be τ for all the N SNs w.l.o.g. The total available bandwidth B is partitioned into K , $K \ll N$ sub-bands and a SN is assumed to operate in the TDD mode. Furthermore, an SN is assigned to only a single sub-band at any given TTI t ; however, multiple SNs can be allocated to the same sub-band. This results in an inter-SN interference scenario. On the other hand, we assume that there is no intra-SN interference. This can be achieved by using a scheduler at the AP, which schedules the UEs in a near-orthogonal fashion [13]. Finally, we model the SN traffic according to an i.i.d Bernoulli random variable w.l.o.g, i.e., a AP either has a packet to transmit or remains idle during a TTI t .

Following operations ensue in a SN to successfully perform LA for DL transmissions. The AP transmits reference signals, which are used to estimate the SINR by the associated UEs either for all K or $\tilde{K} < K$ sub-bands. The estimated SINR is converted to effective signal-to-noise ratio (eSNR) using an effective SNR mapping (ESM) mechanism [14]. The eSNR value is used to prepare the CQI report using predefined look-up tables, which is then sent to the AP in a periodic/apperiodic manner. At the AP, the received CQI is mapped to the corresponding SINR estimate using a look-up table before

¹Recent works [11], [12] also consider SN scenarios with one UE per AP.

performing LA. The SINR estimate of a UE, denoted $\hat{\gamma}_n$, can be written as:

$$\hat{\gamma}_n(t) := \frac{S_n(t)}{I_n(t) + \sigma_w^2}, \quad (1)$$

where, $S_n(t)$ denotes the signal power, which is a function of the wireless channel in the n^{th} SN. The quantity σ_w^2 is the receiver noise power, which is assumed to be same for all UEs w.l.o.g. Finally, $I_n(t)$ is the inter-SN IPV perceived by the N^{th} AP.

In this work, we model $I_n(t)$ based on the spatially consistent 3GPP channel model [15], and formally express it as:

$$I_n(t) := \sum_{n' \in \hat{\mathcal{N}}(t) \setminus \{n\}} \chi_{n'}(t) \cdot P_{n'}(t) \cdot \left(\beta |H_{\text{LOS},n'}(t)|^2 + \sqrt{(1 - \beta^2)} |H_{\text{NLOS},n'}(t)|^2 \right), \quad (2)$$

where, $\hat{\mathcal{N}}(t) \subset \mathcal{N}$ denotes the set of all SNs operating in the same sub-band at TTI t . The quantity $\chi_{n'}(t) \sim \text{Ber}(\rho)$ denotes the ON-OFF traffic parameterized by probability ρ . The term $P_{n'}(t)$ denotes the transmit power of the interfering SNs. Furthermore, $H_{\text{LOS},n'}(t) := h_{\text{LOS},n'}(t) \cdot l_{\text{LOS},n'}(t) \cdot \zeta_{\text{LOS},n'}(t)$ is the consolidated line-of-sight (LOS) channel where $h_{\text{LOS},n'}$ is the small-scale fading co-efficient correlated across TTIs and following Rician pdf [16]; $l_{\text{LOS},n'}$ is the path loss component [15] and $\zeta_{\text{LOS},n'}$ represents the spatially correlated shadowing effect, which follows a log-normal pdf [17]. The value $H_{\text{NLOS},n'}$ is the consolidated non-line-of-sight (NLOS) channel defined in a way similar to the LOS channel. The correlated small scale fading across TTI with rayleigh pdf is denoted as $h_{\text{NLOS},n'}$, alongside path loss $l_{\text{NLOS},n'}$ and shadowing $\zeta_{\text{NLOS},n'}$ with respective NLOS parameters. The parameter $\beta \in (0, 1)$ is a smoothing factor which prevents abrupt fluctuations in the channel response caused by transitions between LOS and NLOS conditions [15]. With the system model in place, we present the problem description in the following section.

III. LINK ADAPTATION PROBLEM

The LA problem involves appropriate MCS selection subject to reliability constraints. As mentioned in section II, an AP performs MCS selection based on the CQI report received from its associated UE. Formally, the LA problem for the UE of the n^{th} SN at TTI t can be expressed as:

$$\lambda_n^*(t) | \hat{\gamma}_n(t) = \sup \{ R(\lambda_n(t)) | \varepsilon(\lambda_n(t)) \leq \bar{\varepsilon} \}, \quad (3)$$

where, $\lambda_n^*(t) \in \mathcal{L}$ is the optimal MCS value with $\mathcal{L}, |\mathcal{L}| = L$ being the set of all feasible MCS values. The quantity $R(\cdot)$ denotes the achievable ergodic rate of UE of n^{th} AP. Finally $\varepsilon(t)$ and $\bar{\varepsilon}$ represent the achieved block error rate (BLER) and target BLER values, respectively.

Following practical challenges arise while solving (3):

- (a) The interference experienced by UEs is not sufficiently reflected in (3) due to both compression losses involved

in ESM and the limited quantization levels collectively characterizing the CQI report.

- (b) Secondly, an AP is more likely to perform MCS selection based on outdated CQI and subsequently the interference information due to inherent protocol overhead and transmission delays involved.

While (a) and (b) are not just specific to LA for SNs, not accounting for them in (3) can have a detrimental effect on the overall latency and reliability requirements, especially in SNs. A straightforward way to include interference information in (3) is by explicitly estimating the IPV's at an UE and sending them back to the associated AP. However, this is impractical in ultra dense SN scenarios since it introduces additional signalling and computational overhead. In this work, we resort to an online signalling-free interference prediction scheme by exploiting the CQI available at the AP, which we describe in the next section.

IV. STATE SPACE MODELING

Prior to discussing the proposed interference prediction scheme, we first present the relevant DSSM of IPV's modeled at the AP w.r.t the CQI reports of the associated UEs. A DSSM deals with time-dependent problems involving latent variables which effectively describes the evolution in the state of the underlying system. Typically, these latent variables are associated with a set of observations. In this work, we model the IPV's as the state/latent variables of the DSSM. This is possible since the CQI report implicitly captures the interference information, even when it is subjected to protocol delays, compression losses and modeling perturbations. Secondly, IPV's demonstrate correlation across TTIs due to the underlying channel model as shown in (2). This is helpful in characterizing the state/latent variable transitions. Given this context, we model a discrete-time Gaussian DSSM at the n^{th} AP, which is formally expressed as follows:

$$I_n(t) := F(I_n(t-1)) + \nu(t), \quad \nu(t) \sim \mathcal{N}(0, \sigma_F^2) \quad (4a)$$

$$Y_n(t) := G(I_n(t)) + u(t), \quad u(t) \sim \mathcal{N}(0, \sigma_G^2). \quad (4b)$$

Here, (4a) represents a process model describing the dynamic evolution of the IPV over the TTIs modeled as the state/latent variable of the DSSM. Similarly, (4b) corresponds to a measurement model relating the CQI report of the associated UE, $Y_n(t)$ to the IPV, $I_n(t)$. The function $F(\cdot)$ denotes the IPV transitions from one TTI to another, whereas $G(\cdot)$ is the observation function represented by SINR (1). The quantity $\nu(t)$ models the process noise in (4b). Similarly, $u(t)$ corresponds to the measurement noise which is jointly characterized w.r.t the error due to compression losses of ESM and CQI quantization. Both $\nu(t)$ and $u(t)$ are assumed to follow a Gaussian pdf with variance σ_F^2 and σ_G^2 , respectively. Although the CQI reporting delay is considered to be one TTI in (4), it can be easily accounted for with minimal modifications to (4a). Given this DSSM, we are interested in mapping $Y_n(t)$ to an estimate of IPV i.e., $\hat{I}_n(t)$ at every t in

an online fashion — a process usually referred to as *filtering* or *online state recovery* in the DSSM literature.

V. EXTENDED KALMAN FILTER APPROXIMATIONS

EKF is a popular Kalman Filter heuristic used for solving the non-linear filtering problem of a DSSM. The EKF, at every prediction instance, provides an instantaneous state estimate based on the observations. To achieve this, the EKF operates on linear approximations of the functions characterizing transition dynamics and/or the observations. In this section, we present the necessary approximations to (4) such that the EKF can be efficiently used for IPV prediction, which is in-turn used for LA improvements. To this extent, we first exploit the correlated nature of small-scale fading coefficients to approximate the transition dynamics of $F(\cdot)$ in (4a). More specifically, we identify that the correlation factor of $h_{NLOS,n}$, $\forall n \in \hat{N}(t)$ in (2) can be approximated using a zeroth-order Bessel function, $B_0(\omega_n \cdot \tau)$ [16]. Here, $\omega_n = 2\pi f_{d_n}$ denotes the Doppler spread, with f_{d_n} being the Doppler frequency and τ being the TTI duration of the interfering SNs as described in section II. Based on this, we approximate the correlation factor of IPV, $\alpha_{F_n} \in (0, 1)$ as follows:

$$\alpha_{F_n} = \frac{1}{N} \sum_N B_0(\omega_n \cdot \tau). \quad (5)$$

Additionally, instead of simply using the previous estimate $\hat{I}_n(t-1)$, we reinforce the EKF prediction by adopting the correlation matching criterion [18]. Formally, this can be represented as a convex combination of the past two predicted IPV, i.e., $\hat{I}_n(t-1)$ and $\hat{I}_n(t-2)$. With a slight abuse of notation in the TTI index representation, we denote the consolidated previous IPV estimate as $\tilde{I}_n(t-1)$. In summary, the linear approximation of the transition dynamics $\tilde{F}(\cdot)$, can be expressed as follows:

$$\tilde{F}(\tilde{I}_n(t-1)) \approx \alpha_{F_n} \cdot \hat{I}_n(t-1) + (1 - \alpha_{F_n}) \cdot \hat{I}_n(t-2). \quad (6)$$

On the other hand, we follow a straightforward approximation of $G(\cdot)$ in (4b) by taking the partial derivative of the $\hat{\gamma}_n(t)$ from (1) w.r.t the IPV estimate, $\hat{I}_n(t)$. In a practical situation where the function characterizing CQI-SINR mapping at the AP is not available, an equivalent approximation for a UE's signal power, S_n can be used in the numerator of (1) for an appropriate representation of $G(\cdot)$. Moreover, the moments of the joint distribution characterizing $u(t)$ are hard to obtain in practical real-time SNs. Thus, we approximate $u(t)$ with a product of two marginal Gaussian random variables associated with, $u_1(t)$, the error in ESM and $u_2(t)$, the CQI quantization function, respectively. We denote this approximated random variable as $\tilde{u}(t)$, whose variance is given by [19]:

$$\tilde{\sigma}_G^2 = \frac{\sigma_{G_1}^2 \cdot \sigma_{G_2}^2}{\sigma_{G_1}^2 + \sigma_{G_2}^2}, \quad (7)$$

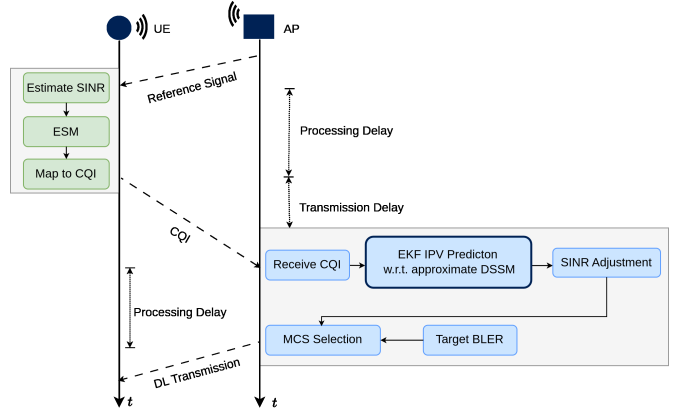


Fig. 2: LA adjustments with IPV prediction

where $\sigma_{G_1}^2$ and $\sigma_{G_2}^2$ denotes the variance associated with $u_1(t)$ and $u_2(t)$, respectively.

We would like to highlight that the key novelty of this work lies in modeling the DSSM for online prediction of IPV and the subsequent approximations for the DSSM to efficiently employ the standard EKF algorithm. Hence, we omit the algorithmic details of the EKF algorithm for brevity. That said, given the approximations of the functions associated with process and measurement models and the corresponding noise variance, the EKF algorithm follows a standard two-step process involving a prediction and an update step [20]. The prediction step outputs an IPV estimate and conditional variance based on $\tilde{F}(\tilde{I}_n(t-1))$. Similarly, in the update step, the approximate moments are propagated to rectify the IPV estimate based on CQI as the observations. Once the IPV estimate is obtained, the SINR estimate is adjusted before performing the LA. The overall LA operation is illustratively summarized in Fig. 2 with the proposed IPV prediction highlighted in blue.

A. Baseline Methods

Following baseline methods are considered for comparison in this work:

- 1) *Genie LA*: This baseline performs MCS selection based on the target BLER $\bar{\epsilon}$ under the assumption that a UE's SINR is perfectly available at the AP. Note that Genie LA is impractical and is considered here as an upper bound for MCS selection [21].
- 2) *Moving-average (MA) Predictor*: In this conventional baseline (used in [5] and [9]), the IPV at TTI t is obtained as a weighted-sum of IPV estimates from TTIs $t-1$ and $t-2$. An important drawback of this baseline is that computing the IPV estimates require explicit channel measurements from the interfering devices.
- 3) *LSTM Predictor*: In this supervised learning based baseline, a pre-trained LSTM model predicts IPV at each t based on a predefined window of previously predicted IPV as its input. This baseline is synonymous to a data-

TABLE I: Simulation Parameters

| Parameter | Value |
|--|---------------------------------|
| Deployment Parameters | |
| Number of SNs, N | 16 |
| Number of UEs, M | 1 |
| Interfering SNs, $ \hat{N}(t) $ | 4 |
| Deployment Area | $20 \times 20 \text{ m}^2$ |
| Minimum separation distance, | 4 m |
| Mobility Model | Random Directional Model |
| Cell Radius, r | 2 m |
| Velocity, v | 2 m/s |
| Channel and PHY Parameters | |
| Carrier frequency | 6 GHz |
| Number of sub-bands, K | 4 |
| Frequency reuse | 1/4 |
| Pathloss | 3GPP InF-DL [22] |
| Shadow fading std. deviation | 4 dB(LOS) 7.2 dB(NLOS) |
| Decorrelation distance, | 10 m |
| Doppler frequency, f_{d_n} | 80 Hz |
| Transmit Power | 0 dBW |
| TTI duration | 0.1 ms |
| Packet size | 160 bits |
| DSSM and EKF Parameters | |
| CQI type | wideband |
| MCS reference table | Table 5.1.3.1 – 3 [23] |
| Number of MCS levels, L | 29 |
| SINR min-max difference, Δ | 4.8 |
| ESM error variance, $\sigma_{G_1}^2$ | $\Delta^2 / (12 \times L)$ [24] |
| CQI mapping error variance, $\sigma_{G_2}^2$ | 2×10^{-9} |
| Noise Factor, | 10 dB |
| Noise Bandwidth, | 50 MHz |
| Process Noise Variance, σ_p^2 | 0.0042 |
| Baseline Parameters | |
| Moving-avg. smoothing factor | 0.01 |
| LSTM sliding window | 30 |
| LSTM prediction-step | 1 |
| LSTM training epochs | 200 |

driven Wiener-filtering method. Refer to [8] for the neural network architecture details.

VI. NUMERICAL RESULTS

In this section, we present the performance evaluation of the proposed approach w.r.t LA improvements and compare it with the baseline methods using numerical simulation results. All relevant simulation parameters considered in this section are summarized in Table I.

In Fig. 3, we first compare the prediction error performance for the proposed method w.r.t the baseline methods. To do so, we use the relative absolute error (RAE) metric defined by:

$$\text{RAE}(t) = |(I_n(t) - \hat{I}_n(t)) / I_n(t)|, \quad (8)$$

where, $I_n(t)$ denotes the reference IPV and $\hat{I}_n(t)$ is the predicted IPV. One can observe that EKF clearly outperforms the moving-average predictor by achieving approximately 8dB lower prediction error. This can be attributed to the fact that the moving-average predictor is not able to track the non-linear dynamics of interference accurately. One can also observe that despite being an unsupervised AP-side method, the prediction error performance of EKF and the *pre-trained* LSTM baseline are almost comparable. This is possible because of the most suitable approximations considered for EKF in Section V.

In Fig. 4 and 5, we evaluate the performance of the proposed EKF in terms of the BLER achieved by MCS selection. Here,

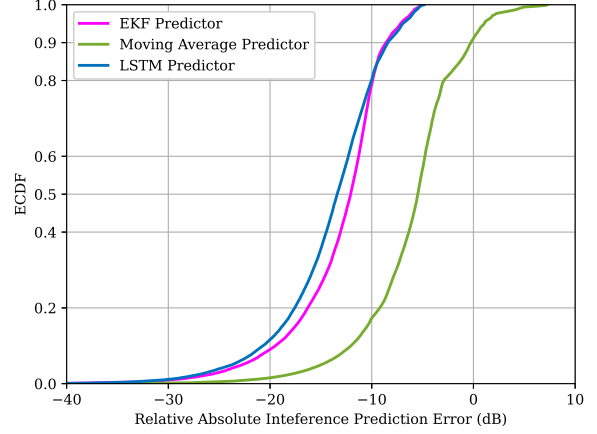


Fig. 3: Empirical cumulative distribution function (ECDF) of RAE

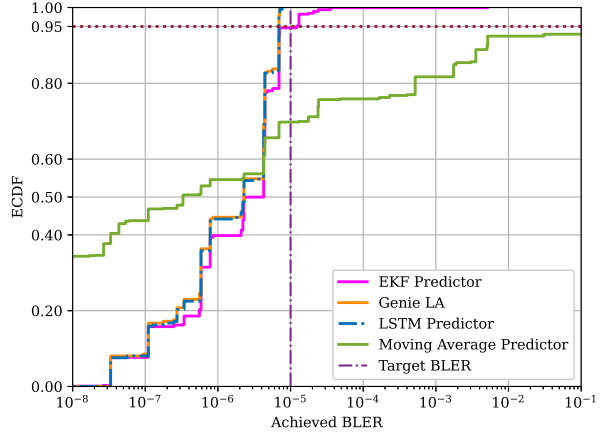


Fig. 4: ECDF of achieved BLER

the achievable BLER is computed based on MCS selection and the reference SINR lookup table mentioned in Table I. In spite of performing prediction solely based on CQI values in an unsupervised manner, proposed EKF achieves a target BLER of $\bar{\varepsilon} = 10^{-5}$ for 95% of the times. Moreover, the performance of EKF predictor strongly matches with that of LSTM and Genie LA baseline methods. This behaviour can be attributed to meticulous approximations w.r.t the interference modeling in (2) and the transition dynamics in (6).

Finally, in Fig. 5, we evaluate the EKF predictor with respect to the Genie LA by varying the target BLER. Our findings indicate that as the target BLER increases, the EKF predictor achieves it within a slight margin of 95% percentile. While the LSTM-based predictor may offer slightly better performance, the EKF predictor presents itself as a computationally inexpensive approach suitable for small form-factor SN devices.

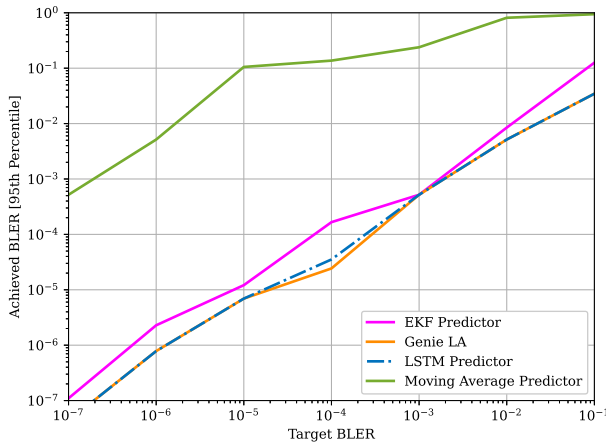


Fig. 5: Achieved BLER for varying target BLER

VII. CONCLUSIONS

In this work, we propose an online and unsupervised interference prediction technique, the EKF predictor, capable of inferring and predicting dynamic interference based on available channel information — specifically, the CQI at a SN. Despite being online and unsupervised method, the performance in terms of prediction error is comparable with LSTM and optimal LA, despite discrepancies in selecting variances associated with quantization, compression, and reconstruction. This suggests that with appropriate modeling and approximations, the proposed low-complexity state-space modeling has the potential to achieve a comparable performance w.r.t machine learning methods. Finally, the vector-valued DSSM capturing multiple UEs per a SN AP along with unknown noise characteristics remain an open topic and needs further investigation.

REFERENCES

- [1] M. Hoffmann, G. Kunzmann, T. Dudda, R. Irmer, A. Jukan, G. Macher, A. Ahmad, F. R. Beenen, A. Bröring, F. Fellhauer *et al.*, “A Secure and Resilient 6G Architecture Vision of the German Flagship Project 6G-ANNA,” *IEEE Access*, vol. 11, pp. 102 643–102 660, 2023.
- [2] G. Berardinelli, P. Baracca, R. O. Adeogun *et al.*, “Extreme Communication in 6G: Vision and Challenges for ‘in-X’ Subnetworks,” *IEEE Open Journal of the Communications Society*, vol. 2, pp. 2516–2535, 2021.
- [3] ITU-R, “Framework and overall objectives of the future development of IMT for 2030 and beyond,” *International Telecommunication Union (ITU) Recommendation (ITU-R)*, 2023.
- [4] M. Ramezani-Mayiami, J. Mohammadi, S. Mandelli, and A. Weber, “CQI Prediction via Hidden Markov Model for Link Adaptation in Ultra Reliable Low Latency Communications,” in *WSA 2021; 25th International ITG Workshop on Smart Antennas*, 2021, pp. 1–5.
- [5] G. Pocovi, K. I. Pedersen, and P. Mogensen, “Joint Link Adaptation and Scheduling for 5G Ultra-Reliable Low-Latency Communications,” *IEEE Access*, vol. 6, pp. 28 912–28 922, 2018.
- [6] A. Brighente, J. Mohammadi, and P. Baracca, “Interference distribution prediction for link adaptation in ultra-reliable low-latency communications,” in *2020 IEEE 91st Vehicular Technology Conference (VTC2020-Spring)*, 2020, pp. 1–7.

- [7] P. Gautam, C. Bockelmann, and A. Dekorsy, “Interference Prediction in Unconnected In-X Mobile 6G Subnetworks Using a Data-Driven Approach,” in *2024 IEEE International Conference on Communications Workshops (ICC Workshops)*, 2024, pp. 2046–2052.
- [8] P. Gautam, M. Vakiliifard, C. Bockelmann, and A. Dekorsy, “Cooperative Interference Estimation Using LSTM-Based Federated Learning for In-X Subnetworks,” in *GLOBECOM 2023 - 2023 IEEE Global Communications Conference*, 2023, pp. 1338–1344.
- [9] N. H. Mahmood, O. A. López, H. Alves, and M. Latva-Aho, “A Predictive Interference Management Algorithm for URLLC in Beyond 5G Networks,” *IEEE Communications Letters*, vol. 25, no. 3, pp. 995–999, 2021.
- [10] X. Xu, M. Ni, and R. Mathar, “Improving QoS by predictive channel quality feedback for LTE,” in *21st International Conference on Software, Telecommunications and Computer Networks - (SoftCOM 2013)*, 2013, pp. 1–5.
- [11] S. Bagherinejad, T. Jacobsen, N. K. Pratas, and R. O. Adeogun, “Comparative Analysis of Sub-band Allocation Algorithms in In-body Sub-networks Supporting XR Applications,” *arXiv preprint arXiv:2403.11891*, 2024.
- [12] R. Adeogun and G. Berardinelli, “Multi-Agent Dynamic Resource Allocation in 6G in-X Subnetworks with Limited Sensing Information,” *Sensors*, vol. 22, no. 13, 2022.
- [13] S. Kapoor, S. Sree Kumar, and S. R. B. Pillai, “Distributed scheduling in multiple access with bursty arrivals under a maximum delay constraint,” *IEEE Transactions on Information Theory*, vol. 64, no. 2, pp. 1297–1316, 2018.
- [14] G. Pocovi, B. Soret, K. I. Pedersen, and P. Mogensen, “MAC layer enhancements for ultra-reliable low-latency communications in cellular networks,” in *2017 IEEE International Conference on Communications Workshops (ICC Workshops)*, 2017, pp. 1005–1010.
- [15] 3GPP, “5G: Study on channel model for frequencies from 0.5 to 100 GHz (Release 16),” 3rd Generation Partnership Project, Tech. Rep. 38.901 v16.1.0, 2020.
- [16] C. Xiao, Y. R. Zheng, and N. C. Beaulieu, “Novel Sum-of-Sinusoids Simulation Models for Rayleigh and Rician Fading Channels,” *IEEE Transactions on Wireless Communications*, vol. 5, no. 12, pp. 3667–3679, 2006.
- [17] S. Lu, J. May, and R. J. Haines, “Effects of correlated shadowing modeling on performance evaluation of wireless sensor networks,” in *2015 IEEE 82nd Vehicular Technology Conference (VTC2015-Fall)*, 2015, pp. 1–5.
- [18] S. Ghandour-Haidar, L. Ros, and J.-M. Brossier, “On the use of first-order autoregressive modeling for Rayleigh flat fading channel estimation with Kalman filter,” *Signal Processing*, vol. 92, no. 2, pp. 601–606, 2012.
- [19] P. A. Bromiley, “Products and convolutions of Gaussian distributions,” *Medical School, Univ. Manchester, Manchester, UK, Tech. Rep.*, vol. 3, 2003.
- [20] S. M. Kay, *Fundamentals of statistical signal processing: estimation theory*. Prentice-Hall, Inc., 1993.
- [21] M. Alonzo, P. Baracca, S. R. Khosravirad, and S. Buzzi, “URLLC for Factory Automation: an Extensive Throughput-Reliability Analysis of D-MIMO,” in *WSA 2020; 24th International ITG Workshop on Smart Antennas*, 2020, pp. 1–6.
- [22] 3GPP, “Study on Communication for Automation in Vertical Domains (Release 16),” 3rd Generation Partnership Project, Tech. Rep. 22.804 v1.2.0, 2018.
- [23] 3GPP, “Physical layer procedures for data (Release 16),” 3rd Generation Partnership Project, Tech. Rep. 38.214 v16.2.0, 2020.
- [24] R. L. Easton, *Fundamentals of digital image processing*, 2010.